

Expression for the heavy-ion fusion cross section

V. Yu. Denisov 

INFN Laboratori Nazionali di Legnaro, Viale dell'Università 2, 35020 Legnaro, Italy;
Institute for Nuclear Research, Prospect Nauki 47, 03028 Kiev, Ukraine;
and Faculty of Physics, Taras Shevchenko National University of Kiev, Prospect Glushkova 2, 03022 Kiev, Ukraine



(Received 21 April 2023; accepted 23 May 2023; published 30 May 2023)

The expression for calculation of the heavy-ion fusion cross section is obtained in the case of approximation of the total heavy-ion potential around the barrier by the Morse potential. The approximation of the total heavy-ion potential around the barrier by the Morse potential is more realistic than the parabolic one. The asymptotic expressions of the fusion cross section at sub-barrier energies obtained for the Morse and parabolic approximations of the total heavy-ion potential have different dependencies on collision energy. The fusion cross sections calculated for the Morse and parabolic approximations of the total heavy-ion potential are discussed for the reactions $^{12}\text{C} + ^{24}\text{Mg}$ and $^{12}\text{C} + ^{30}\text{Si}$ in detail.

DOI: [10.1103/PhysRevC.107.054618](https://doi.org/10.1103/PhysRevC.107.054618)

I. INTRODUCTION

The study of fusion reactions at sub-barrier energies has seen an increased interest in recent years [1–17]. The fusion process has been assumed to occur if colliding nuclei either penetrate or overcome the total potential barrier formed due to Coulomb, nuclear, and centrifugal forces.

The total heavy-ion potential around the barrier is often approximated by parabolic barrier [1–3,8,9,12,17]. There is an exact expression for the transmission coefficient through the parabolic barrier [18,19]. By using this expression for the transmission coefficient, Wong obtained a simple expression for the heavy-ion fusion cross section [1]. This expression is very widely applied for the analysis of the heavy-ion fusion cross section, see, for example, Refs. [1–3,8,9,12,17] and papers cited therein. There are other simple expressions for the heavy-ion fusion cross section [10,12,14].

The parabolic approximation of the total potential around the barrier is symmetric relative to the barrier distance, see Fig. 1. However, the realistic total heavy-ion potential is strongly asymmetric around the barrier distance r_b . The total potential is drastically decreasing at distances $r < r_b$ due to the exponential increase of the contribution of the nuclear part of the ion-ion potential with decreasing of r [20–26]. At distances $r > r_b$ the potential decreases as $1/r$ due to the exponential decrease of the nuclear part of ion-ion potential and the leading role of the Coulomb potential. The asymmetric shape of the ion-ion potential may be approximated by the Morse potential [27], see Fig. 1 and Refs. [9,17]. The shape of the Morse potential is closer to the shape of the realistic total potential than the parabolic one.

Ahmed obtained the exact expression for the transmission coefficient through the Morse barrier [28]. Therefore, it is very useful to get the expression for the heavy-ion fusion cross section for the Morse potential using the same approximations as in the case of Wong formula [1]. Such analytical formula is derived in the next section. Note, the goal is to obtain the

analytical formula for the heavy-ion fusion cross section based on the Morse approximation of the total potential. Due to this any coupled-channel effects on the fusion cross section, which are important [2–8,13,16], are not considered. The comparison of the results of the cross-section calculations using the new and Wong formulas is given in Sec. III. The conclusions are given in Sec. IV.

II. EXPRESSIONS FOR THE HEAVY-ION FUSION CROSS SECTION

The heavy-ion fusion cross section [1–10,12–14,16,17] is given by

$$\sigma(E) = \frac{\pi \hbar^2}{2\mu E} \sum_{\ell=0}^{\infty} (2\ell + 1) T_{\ell}(E), \quad (1)$$

where μ is the reduced mass, E is the energy of collision in the center of mass system, and $T_{\ell}(E)$ is the transmission coefficient through the total interaction potential barrier formed by the Coulomb $V_C(r)$, nuclear $V_N(r)$, and centrifugal $V_{\ell}(r)$ potential energies of two nuclei. The nuclear part of the potential is often parametrized by the Woods-Saxon potential [20,23,26]. As a result, the total interaction potential energy of two spherical nuclei for the partial wave ℓ can be presented in the form

$$\begin{aligned} V_{\ell}(r) &= V_C(r) + V_N(r) + V_{\ell}(r) \\ &= \frac{Z_1 Z_2 e^2}{r} - \frac{V_{WS}}{1 + \exp[(r - r_{WS})/d_{WS}]} + \frac{\hbar^2 \ell(\ell + 1)}{2\mu r^2}. \end{aligned} \quad (2)$$

Here, Z_1 and Z_2 are the numbers of protons in the interacting nuclei, e is the charge of the proton, and V_{WS} , r_{WS} , and d_{WS} are the parameters of the Woods-Saxon potential.

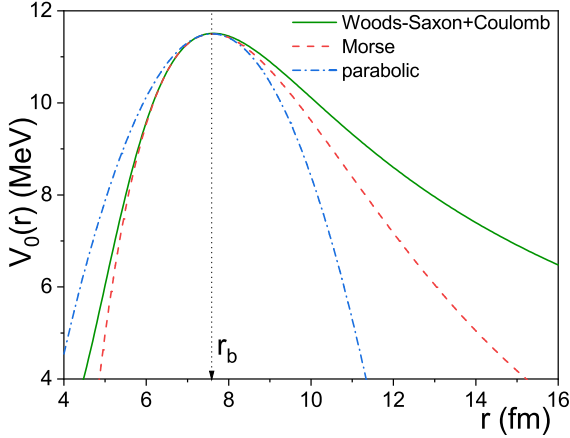


FIG. 1. The comparison of the total potential for $\ell = 0$ (Woods-Saxon+Coulomb) with the Morse and parabolic approximations of the total potential around barrier for the system $^{12}\text{C} + ^{24}\text{Mg}$. The barrier height, radius (r_b), and curvature for all potentials are the same.

A. The fusion cross section in the case of parabolic barrier

Let the total interaction potential energy of two nuclei for the partial wave ℓ be approximated by the parabolic function around the barrier as

$$V_\ell^p(r) \approx B_\ell + \frac{\hbar^2 \ell(\ell+1)}{2\mu r_\ell^2} - \frac{\mu \omega_\ell^2 (r - r_\ell)^2}{2}. \quad (3)$$

Here, $B_\ell + \frac{\hbar^2 \ell(\ell+1)}{2\mu r_\ell^2}$, r_ℓ , and $\hbar\omega_\ell$ are, respectively, the height, radius, and curvature of the barrier. Then, using the Kemple-Hill-Wheeler formula [18,19] for the transmission coefficient $T_\ell(E)$ through a parabolic barrier, the cross section is given as

$$\sigma(E) = \frac{\pi \hbar^2}{2\mu E} \sum_{\ell=0}^{\infty} \frac{(2\ell+1)}{1 + \exp\left[\frac{2\pi}{\hbar\omega} \left(B_\ell + \frac{\hbar^2 \ell(\ell+1)}{2\mu r_\ell^2} - E\right)\right]}. \quad (4)$$

Taking B_ℓ , r_ℓ , $\hbar\omega_\ell$ as fixed at the partial wave $\ell = 0$, and replacing the summation by an integral, one obtains the Wong formula [1] for the fusion cross section

$$\sigma_W(E) = \frac{r_b^2 \hbar\omega}{2E} \ln \{1 + \exp[2\pi(E - B)/\hbar\omega]\}. \quad (5)$$

Here, $r_0 = r_b$ and $B = B_0$ are, respectively, the radius and height of the barrier for the partial wave $\ell = 0$, and

$$\hbar\omega \equiv \hbar\omega_0 = \left(-\frac{\hbar^2}{\mu} \frac{d^2 V_0(r)}{dr^2} \right)^{1/2} \Big|_{r=r_b} \quad (6)$$

is the curvature of the total potential for $\ell = 0$. Emphasize that the Wong formula for the fusion cross section is obtained in the assumptions that B_ℓ , r_ℓ , ω_ℓ are rather insensitive to ℓ .

B. The fusion cross section in the case of heavy-ion potential approximated by the Morse potential

Applying the independence of B_ℓ , r_ℓ , ω_ℓ on ℓ , the total interaction potential energy of two spherical nuclei for the partial wave ℓ can be approximated around the barrier by the

Morse potential

$$V_\ell^M(r) \approx \left(B + \frac{\hbar^2 \ell(\ell+1)}{2\mu r_b^2} \right) \left[2 \exp\left(-\frac{r-r_b}{d}\right) - \exp\left(-2\frac{r-r_b}{d}\right) \right]. \quad (7)$$

Then, using the Ahmed formula [28] for the transmission coefficient $T_\ell(E)$ through the Morse barrier, the cross section is given as

$$\sigma(E) = \frac{\pi \hbar^2}{2\mu E} \sum_{\ell=0}^{\infty} \frac{(2\ell+1)[1 - \exp(-4\pi\alpha)]}{1 + \exp[2\pi(\beta_\ell - \alpha)]}, \quad (8)$$

where

$$\alpha = \left(\frac{2\mu d^2 E}{\hbar^2} \right)^{1/2}, \quad (9)$$

$$\beta_\ell = \left[\frac{2\mu d^2}{\hbar^2} \left(B + \frac{\hbar^2 \ell(\ell+1)}{2\mu r_b^2} \right) \right]^{1/2}. \quad (10)$$

Equations (4) and (8) are very similar.

As pointed out in Ref. [28] the contribution of the term $\exp(-4\pi\alpha)$ in the Ahmed transmission coefficient is negligible. Neglecting this term in Eq. (8) and replacing the summation on ℓ by an integral, one obtains the formula for the heavy-ion fusion cross section for the potential barrier (7) in the form

$$\sigma(E) = \frac{\pi r_b^2 (\hbar\omega_M)^2}{4EB} \left[\frac{\text{Li}_2[-\exp(-2\pi(\alpha - \beta_0))]}{2\pi^2} + \frac{\ln[1 + \exp(-2\pi(\alpha - \beta_0))]\beta_0}{\pi} + \alpha^2 - \beta_0^2 + \frac{1}{12} \right]. \quad (11)$$

Here, $\text{Li}_2(x)$ is the dilogarithm function [29–32]. The curvature of the Morse potential barrier for $\ell = 0$ is

$$\hbar\omega_M = \left(-\frac{\hbar^2}{\mu} \frac{d^2 V_0^M(r)}{dr^2} \right)^{1/2} \Big|_{r=r_b} = \left(\frac{\hbar^2}{\mu} \frac{2B}{d^2} \right)^{1/2}. \quad (12)$$

If the parabolic and Morse potentials are used for the approximation of the same total potential (2) then $\hbar\omega_M = \hbar\omega$.

Using Eq. (12) the parameters α and β_0 can be presented as the functions of B , E , and $\hbar\omega$:

$$\alpha = \frac{2(BE)^{1/2}}{\hbar\omega}, \quad (13)$$

$$\beta_0 = \frac{2B}{\hbar\omega}. \quad (14)$$

Substituting Eqs. (13)–(14) into Eq. (11) the expression for the heavy-ion fusion cross section is presented in the simple form

$$\sigma(E) = \pi r_b^2 \left\{ 1 - \frac{B}{E} + \frac{(\hbar\omega)^2}{48BE} + \frac{\hbar\omega}{2\pi E} \ln[1 + \exp(4\pi(B - \sqrt{BE})/\hbar\omega)] + \frac{(\hbar\omega)^2}{8\pi^2 BE} \text{Li}_2[-\exp(4\pi(B - \sqrt{BE})/\hbar\omega)] \right\}. \quad (15)$$

So, Eqs. (5) and (15) for the heavy-ion fusion cross section depend on the same characteristics of the total heavy-ion potential (2) near the barrier, which are the barrier height B , radius r_b , and curvature $\hbar\omega$.

III. DISCUSSION

Let us consider the asymptotic behavior of the expressions for the heavy-ion fusion cross sections in the case of high and low collision energies in comparison to the fusion barrier height B . The asymptotic dependencies of the Wong formula are well known:

$$\sigma_W(E) \approx \begin{cases} \pi r_b^2 \left(1 - \frac{B}{E}\right), & \text{if } 2\pi \frac{E-B}{\hbar\omega} \gg 1, \\ \frac{r_b^2 \hbar\omega}{2E} \exp\left(2\pi \frac{E-B}{\hbar\omega}\right), & \text{if } 2\pi \frac{E-B}{\hbar\omega} \ll -1. \end{cases} \quad (16)$$

The asymptotic dependencies of the formula (15) are

$$\sigma(E) \approx \begin{cases} \pi r_b^2 \left(1 - \frac{B}{E} + \frac{(\hbar\omega)^2}{48BE}\right), & \text{if } 4\pi \frac{\sqrt{BE}-B}{\hbar\omega} \gg 1, \\ \frac{r_b^2 \hbar\omega}{2E} \left(1 + \frac{\hbar\omega}{4\pi B}\right) \times \\ \exp\left(4\pi \frac{\sqrt{BE}-B}{\hbar\omega}\right), & \text{if } 4\pi \frac{\sqrt{BE}-B}{\hbar\omega} \ll -1. \end{cases} \quad (17)$$

Here, the properties of the dilogarithm functions [29,30]

$$\text{Li}_2(z) \approx z \text{ at } |z| \ll 1, \quad (18)$$

$$\text{Li}_2(-z) + \text{Li}_2(-1/z) = -\pi^2/6 - (1/2)(\ln z)^2 \quad (19)$$

are taken into account. (Equation (19) was obtained by Euler in 1768 [29].)

The values of the asymptotic cross section for high-energy collisions, $E > B$, in Eqs. (16) and (17) are very similar, because the contribution of the last term in brackets in the corresponding expression of Eq. (17) is small as a rule. In contrast to this, the different dependencies of the cross section on E at sub-barrier energies, $E < B$, are observed for the parabolic and Morse approximation of the barrier. Note that using the asymptotic expression of the cross section at very low-energy collisions may be preferable because the accurate calculation of the dilogarithm function at such a value of an argument is difficult.

It is useful to introduce the parameter $\delta = (E - B)/B$ and apply this parameter for the low-energy asymptotics of the fusion cross section (16) and (17), which are written as

$$\sigma_W(E) \propto \exp\left[\frac{2\pi B\delta}{\hbar\omega}\right], \quad (20)$$

$$\sigma(E) \propto \exp\left[\frac{2\pi B\delta}{\hbar\omega} \left(1 - \frac{\delta}{4} + \frac{\delta^2}{8} + \dots\right)\right]. \quad (21)$$

The ratio of asymptotics of the cross section at the sub-barrier energies is

$$\frac{\sigma_W(E)}{\sigma(E)} \propto \exp\left[\frac{\pi B\delta^2}{2\hbar\omega} \left(1 - \frac{\delta}{2} + \dots\right)\right]. \quad (22)$$

Therefore, the Wong cross section is higher than the cross section evaluated for Morse potential at sub-barrier collision energies. The strong effect on the cross section appears at large values of δ . The large values of δ are taken place at deep sub-barrier collision energies for light-heavy-ion systems with

small values of the barrier height B . Due to this, the reactions $^{12}\text{C} + ^{24}\text{Mg}$ and $^{12}\text{C} + ^{30}\text{Si}$ are considered below for the practical applications of discussed expressions for the heavy-ion fusion cross section.

The fusion cross section for the reaction $^{12}\text{C} + ^{24}\text{Mg}$ calculated using Eqs. (5) and (15) are compared with the experimental data in Fig. 2. The experimental data for the fusion cross section for this reaction are taken from Refs. [15].

The parameters $B = 11.5$ MeV, $r_b = 7.6$ fm, and $\hbar\omega = \hbar\omega_W = 2.36$ MeV are obtained by fitting the experimental fusion cross-section data using Eq. (15). The fitting is done by eye. As an example, these values of parameters for the Akyuz-Winter potential [23] are $B = 11.5$ MeV, $r_b = 8.3$ fm, and $\hbar\omega = 3.23$ MeV. The barrier heights are the same in both cases. The fusion cross section at over-barrier energies is proportional to r_b^2 , see Eqs. (16) and (17). The value $r_b = 7.6$ fm leads to a good description of the over-barrier cross-section values, see Fig. 2. The curvature of the Akyuz-Winter potential is larger than the one obtained in the fusion cross-section fit using Eq. (15).

The experimental fusion cross section is well described by the formula (15) in the full energy range, see Fig. 2. The Wong formula well describes the experimental data around the barrier and at over-barrier collision energies. The cross section calculated with the help of the Wong formula strongly overestimates the experimental cross section at deep sub-barrier energies. The difference between these approaches at sub-barrier energies is due to the larger thickness of the Morse barrier at sub-barrier energies than the one of the parabolic barrier, see Fig. 1. Remember that expressions (5) and (15), as well as the parabolic and Morse approximations of the total potential, are obtained using the same values of the barrier characteristics.

The corresponding parabolic and Morse potentials are compared with the total Coulomb+Woods-Saxon nucleus-nucleus potential $V_0(r)$ for the system $^{12}\text{C} + ^{24}\text{Mg}$ in Fig. 1. The Morse potential is a drastically better fit $V_0(r)$ than the parabolic approximation. The parameters of Woods-Saxon potential $V_{WS} = 38.3$ MeV, $r_{WS} = 4.48$ fm, and $d_{WS} = 1.1$

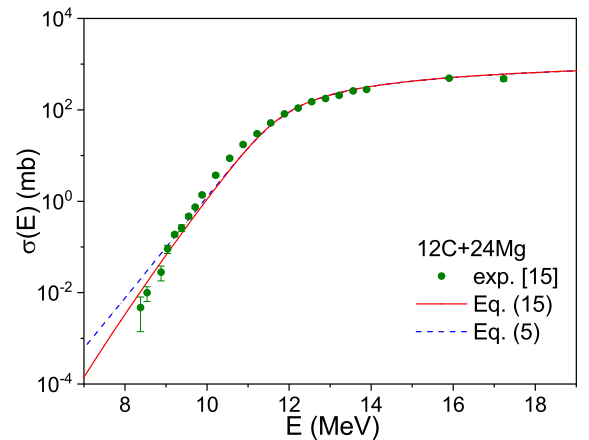


FIG. 2. The comparison of the fusion cross section $\sigma(E)$ for the reaction $^{12}\text{C} + ^{24}\text{Mg}$ evaluated with the help of Eqs. (5) and (15) with experimental data from Ref. [15].

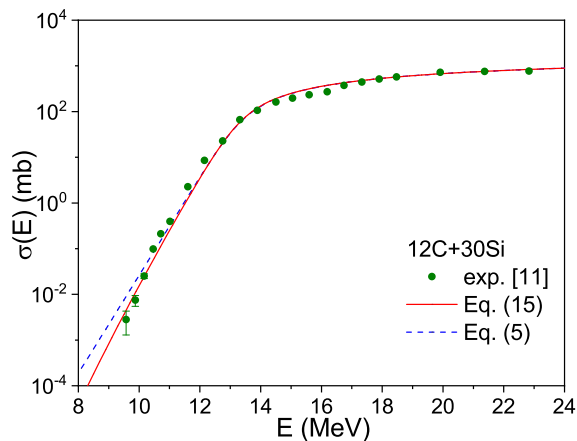


FIG. 3. The comparison of the fusion cross section $\sigma(E)$ for the reaction $^{12}\text{C} + ^{30}\text{Si}$ evaluated with the help of Eqs. (5) and (15) with experimental data from Ref. [11].

fm are obtained by fitting the barrier characteristics B , r_b , and $\hbar\omega$, which are used for the cross-section description with the help of Eq. (15). These values of parameters are different from the corresponding parameters of the Akyuz-Winther potential [23]. Note, that the Akyuz-Winther [23] and other nucleus-nucleus potentials [20–22,24–26] are used in the coupled-channel calculations of the fusion cross section [2–8,13,16]. The effect of coupled-channel enhancement of the fusion cross section below the barrier is modeled by the reduction of the barrier curvature in the present approach.

The fusion cross sections for the reaction $^{12}\text{C} + ^{30}\text{Si}$ calculated using Eqs. (5) and (15) are compared with the experimental data in Fig. 3. The experimental data for the fusion cross section for this reaction are taken from Ref. [11]. The parameters $r_b = 7.9$ fm, $B = 13.1$ MeV, and $\hbar\omega = \hbar\omega_W = 2.44$ MeV are obtained by fitting the experimental cross-section data using Eq. (15). The fusion cross section evaluated with the help of the Morse potential better agree with the experimental data below barrier than the one obtained for the parabolic potential.

In the case of the Morse potential, the heavy-ion fusion cross section can be calculated using the exact expression (8) as well as Eq. (15), which is obtained using in Eq. (8) the replacement of the sum over ℓ by the corresponding integral. The differences between the cross-section values found with the help of Eqs. (8) and (15) are small. As an example, it reaches several percent at deep sub-barrier energies for

reactions considered here. Moreover, this difference decreases with the increase of the collision energy. Therefore, the precision of Eq. (15) is high.

Note, that a detailed comparison of the heavy-ion fusion cross section calculated using the parabolic, Morse, and more realistic Coulomb+Woods-Saxon or double-folding total nucleus-nucleus potentials is discussed in Refs. [9,17]. In the case of the Coulomb+Woods-Saxon or double-folding nucleus-nucleus potential, the fusion cross section is calculated using the Kemble expression for the transmission coefficient related to the direct calculation of the action between the turning points of the total potential [9,17]. Such the semiclassical Wentzel-Kramers-Brillouin approach is traditional for the sub-barrier tunneling [33] and sub-barrier fusion reactions, see, for example, [2,5].

IV. CONCLUSION

The expression for calculation of the heavy-ion fusion cross section is obtained in the case of approximation of the total heavy ion potential around the barrier by the Morse potential. The approximation of the heavy ion potential around the barrier by the Morse potential is more realistic than the parabolic one.

The over-barrier fusion cross sections calculated for the parabolic and Morse potentials at the same values of the barrier height B , radius r_b , and curvature $\hbar\omega$ lead to practically the same cross-section values. In contrast to this, the values of the sub-barrier fusion cross sections obtained with the help of the Morse potential are smaller than the ones for the parabolic barrier. The fusion cross sections obtained for the Morse and parabolic approximations of the total heavy-ion potential have different dependencies on collision energy.

The fusion cross sections obtained using Morse approximations of the total heavy-ion potential better agree with the experimental data for the reactions $^{12}\text{C} + ^{24}\text{Mg}$ and $^{12}\text{C} + ^{30}\text{Si}$ than the parabolic one.

ACKNOWLEDGMENTS

The author thanks the support of Prof. Fabiana Gramegna, Prof. Enrico Fioretto, Prof. Giovanna Montagnoli, and Prof. Alberto Stefanini. The author thanks the support of Istituto Nazionale di Fisica Nucleare, Laboratori Nazionali di Legnaro of Istituto Nazionale di Fisica Nucleare, the National Academy of Sciences of Ukraine and Taras Shevchenko National University of Kiev.

[1] C. Y. Wong, *Phys. Rev. Lett.* **31**, 766 (1973).
 [2] B. Balantekin and N. Tagikawa, *Rev. Mod. Phys.* **70**, 77 (1998).
 [3] M. Dasgupta *et al.*, *Annu. Rev. Nucl. Part. Sci.* **48**, 401 (1998).
 [4] K. Hagino, N. Rowley, and A. T. Kruppa, *Comput. Phys. Commun.* **123**, 143 (1999).
 [5] V. Yu. Denisov, *Eur. Phys. J. A* **7**, 87 (2000).
 [6] B. B. Back, H. Esbensen, C. L. Jiang, and K. E. Rehm, *Rev. Mod. Phys.* **86**, 317 (2014).

[7] V. Yu. Denisov, *Phys. Rev. C* **89**, 044604 (2014).
 [8] G. Montagnoli and A. M. Stefanini, *Eur. Phys. J. A* **53**, 169 (2017).
 [9] A. J. Toubiana, L. F. Canto, and M. S. Hussein, *Braz. J. Phys.* **47**, 321 (2017).
 [10] C. L. Jiang *et al.*, *Eur. Phys. J. A* **54**, 218 (2018).
 [11] G. Montagnoli *et al.*, *Phys. Rev. C* **97**, 024610 (2018).
 [12] V. Yu. Denisov and I. Yu. Sedykh, *Eur. Phys. J. A* **55**, 153 (2019).

- [13] C. L. Jiang *et al.*, *Eur. Phys. J. A* **57**, 235 (2021).
- [14] C. L. Jiang and B. P. Kay, *Phys. Rev. C* **105**, 064601 (2022).
- [15] G. Montagnoli *et al.*, *J. Phys. G: Nucl. Part. Phys.* **49**, 095101 (2022).
- [16] V. Yu. Denisov and I. Yu. Sedykh, *Eur. Phys. J. A* **58**, 91 (2022).
- [17] S. Rana, R. Kumar, S. K. Patra, and M. Bhuyan, *Eur. Phys. J. A* **58**, 241 (2022).
- [18] E. C. Kemble, *Phys. Rev.* **48**, 549 (1935).
- [19] D. L. Hill and J. A. Wheeler, *Phys. Rev.* **89**, 1102 (1953).
- [20] R. Bass, *Nuclear Reactions with Heavy Ions* (Springer, Berlin, 1980).
- [21] J. Błocki *et al.*, *Ann. Phys.* **105**, 427 (1977).
- [22] H. J. Krappe, J. R. Nix, and A. J. Sierk, *Phys. Rev. C* **20**, 992 (1979).
- [23] O. Akyuz and A. Winther, in *Proceedings of the Enrico Fermi School of Physics, 1979*, edited by R. A. Broglia, C. H. Dasso, and R. Ricci, Course on Nuclear Structure and Heavy-Ion Reactions (North-Holland, Amsterdam, 1981), p. 491.
- [24] V. Yu. Denisov, *Phys. Lett. B* **526**, 315 (2002).
- [25] I. Dutt and R. K. Puri, *Phys. Rev. C* **81**, 064608 (2010).
- [26] V. Yu. Denisov, *Phys. Rev. C* **91**, 024603 (2015); V. Yu. Denisov and I. Yu. Sedykh, *Chin. Phys. C* **45**, 044106 (2021); V. Yu. Denisov, *Eur. Phys. J. A* **58**, 188 (2022).
- [27] P. M. Morse, *Phys. Rev.* **34**, 57 (1929).
- [28] Z. Ahmed, *Phys. Lett. A* **157**, 1 (1991).
- [29] A. N. Kirillov, *Prog. Theor. Phys. Suppl.* **118**, 61 (1995).
- [30] D. Zagier, in *The Dilogarithm Function*, edited by P. Cartier, P. Moussa, B. Julia, and P. Vanhove, *Frontiers in Number Theory, Physics, and Geometry II* (Springer, Berlin/Heidelberg, 2006).
- [31] Y. L. Luke, *Mathematical Functions and Their Approximations* (Academic Press, New York, 1975).
- [32] K. S. Kolbig, *Dilogarithm Function*, CERN Program Library, CERN, Geneva, 1996.
- [33] N. Froman and P. O. Froman, *JWKB Approximation* (North-Holland Publishing Company, Amsterdam, 1965).